Vol. 35 No. 9 Transactions of Information Processing Society of Japan Sep. 1994

Regular Paper

Texture Approach to Dynamic Contour Following

ROMAN ĎURIKOVIČ,[†,††] KAZUFUMI KANEDA [†] and HIDEO YAMASHITA [†]

This paper proposes a method for following the contours of an object in an image with a roughly estimated initial contour. The method is based on active contour model which converges the initial contour close to the objects boundary. In general, active contour models are suitable for applications of medical imaging such as extracting contours from images taken by using computed tomography (CT) and magnetic resonance images (MRI). We have found the proposed active contour model very useful in the area of anatomy, where the shape of a mouse embryo organ has to be reconstructed from a set of contours extracted from microscopic images. A texture representation of an image and texture energies in active contour models are utilized, something which is presented for the first time in this paper. The proposed method makes it possible to establish the shape of an object even when complex texture exists in or near the target object.

1. Introduction

Shape encloses information gained from local properties of an image such as texture, topology or color. The problem of distinguishing object shape from its surroundings will be approached as a process of finding boundary using texture feature vectors and incorporating global shape information.

This work aims at segmenting 2D objects from 2D images. The objects are taken from a microscope with problems such as noise and poor contrast. Objects such as embryo organs are expected to tend towards having average texture properties and average shapes. These tendencies can be taken advantage of when designing a set of energies in an active contour model. Our approach is to design energies on a texture space representation of an image. If an object consists of many small cells or a little broken parts (such cases occur often in microscopic images) traditional methods[10] using spatial filters tend to extract edges of those cells and broken parts while the proposed active contour model in conversely has tendency to find the shape of the target object.

The active contour models proposed by Kass et al.[7] and Wang[13] use image space representation for the boundary. These models originally require the object contour to be C^1 continuous. This restriction implies errors in the approximation of C^1 discontinuous boundaries with corners. The setting of models' parameters is another problem. Even if we set parameters for group of images, those parameters may not be valid for other images (with different contrasts). In order to avoid such problems, Etoh et al.[5] provide a mixture density description of an image and its decomposition on sub-regions. This approach is similar to our method but our method is inexpensive in comparison, because they require a computationally demanding region clustering algorithm.

Other investigators have incorporated global shape information. Kita[8] constructed a stomach model, the shape of which was based on and extracted from different types of X-ray images. This method fails in the case of poorly contrasted images and when these are places where the intensity average is almost the same. These boundary finding methods are related to elastic matching methods used for the similar problem of image registration.[1),2)] Shapes with high curvature points or corners are very difficult to extract even with a probabilistic deformable model with flexible constraints, as investigated in Ref. 11). The advantage of the proposed technique, as will be seen, is that the global shape information is described from the texture description of an image, moreover high curvature points and corners can be easily followed.

† Electric Machinery Laboratory, Faculty of Engineering, Hiroshima University, Higashihiroshima, Japan
†† On leave from Department of Computer Graphics and Image Processing, Faculty of Mathematics and Physics, Comenius University, Bratislava, Slovakia

2. Texture Model

A kind of two dimensional noncausal random field model called the "Simultaneous Autoregressive Model", (SAR), has been used by many researchers.[9),6)] In this correspondence we consider the second order SAR model as an appropriate toll for efficient texture description.

Let Ω denote the set of grid points in the $M \times M$ lattice, i.e., $\Omega = \{(x, y), 0 \leq x, y \leq M-1\}$ shown in **Fig. 1**. Let $\{I(x, y), (x, y) \in \Omega\}$ and μ_Ω denote the intensities and mean of the intensities in the lattice, respectively. Let N be the symmetric second order neighborhood of a site, we can write the following expression for gray level $I(x, y)$ and its neighborhood at the pixel site (x, y):

$$I(x, y) - \mu_\Omega = \sum_{(i,j)\in N} \Theta(i, j)[I(x \oplus i, y \oplus j) - \mu_\Omega] + \sqrt{\rho_N}\, w(x, y) \quad (1)$$

where a model parameter $\Theta(i, j)$ indicates the correlation between a site and its neighborhood, ρ_N is noise variance, $w(x, y)$ is a noise sequence approximated by a Gaussian random variable with zero mean and unit variance. The symbol '$\oplus$' means addition in module M.

2.1 SAR Parameter Estimation

Two types of SAR models used in our texture description are defined on two kind of neighborhoods $N_1 = \{(1, 0), (0, 1), (-1, 0), (0, -1)\}$ and $N_2 = \{(1, 1), (-1, 1), (-1, -1), (1, -1)\}$. Our interest is in $\{\Theta(0, 1), \Theta(1, 0), \rho_{N_1}\}$ parameters obtaining the horizontal and vertical texture information from N_1 neighborhood and in $\{\Theta(1, 1), \Theta(-1, 1), \rho_{N_2}\}$ parameters obtaining the diagonal texture information from N_2 neighborhood.

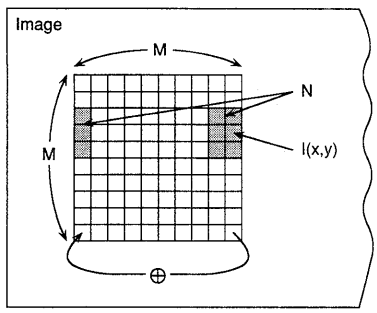

Fig. 1 The neighborhood of a site (x, y) on a lattice $M \times M$. The rolling situation which appears on the lattice borders according to operator $\oplus$ is shown.

There are many existing methods for estimating the SAR parameters, but none of them can guarantee both consistency (estimates converging to the true values of the parameters) and stability (the covariance matrix in Eq. (1) must be positive definite). Normally an optimization algorithm is used to obtain the stable estimates. The parameters of the SAR are used in obtaining certain measures for classification and not for texture synthesis. Thus it is convenient to use computationally less demanding methods which can provide rationally good parameter estimates. A popular method[6)] of estimation is that of least squares.

We consider that the notation $col[A]$ gives us a column representation of matrix A. In this sense we represent the image intensities in neighborhood N as column vector

$$Z(x, y) = col[I(x \oplus i, y \oplus j), (i, j) \in N]. \quad (2)$$

Thus the least squares method yields the estimates $\hat{\Theta}$ and $\hat{\rho_N}$ of the exact parameters Θ and ρ_N by the expressions

$$\hat{\Theta} = [\sum_{x=0}^{M-1}\sum_{y=0}^{M-1} Z(x, y) Z^T(x, y)]^{-1} \cdot (\sum_{x=0}^{M-1}\sum_{y=0}^{M-1} Z(x, y) I(x, y)) \quad (3)$$

$$\hat{\rho_N} = \frac{1}{M^2}\sum_{x=0}^{M-1}\sum_{y=0}^{M-1}(I(x, y) - \hat{\Theta} Z(x, y))^2 \quad (4)$$

where the neighborhood $N = N_1$ or N_2. The consequent estimate $\hat{\Theta}$ is a column vector with elements $\hat{\Theta}(i, j)$ written as

$$\hat{\Theta} = col[\hat{\Theta}(i, j), (i, j) \in N]. \quad (5)$$

Let the μ_Ω be the mean in the lattice. The feature vector for the region Ω is denoted by

$$F = (f_1, f_2, f_3, f_4, f_5, f_6, f_7) \quad (6)$$
$$= (\hat{\Theta}(0, 1), \hat{\Theta}(1, 0), \hat{\Theta}(1, 1), \hat{\Theta}(-1, 1), \hat{\rho_{N_1}}, \hat{\rho_{N_2}}, \mu_\Omega)$$

2.2 Segmentation

In the segmentation process, the image is scanned from top to bottom and from left to right by the $M \times M$ lattice region. The lattice regions cover the image in d-pixel wide steps both horizontally and vertically, overlapping each other to smooth the borders between texture regions. For each of these regions, we calculate the feature vector. The places where texture features will vary dramatically are edge locations of different regions.

A normalized Euclidean distance measure is

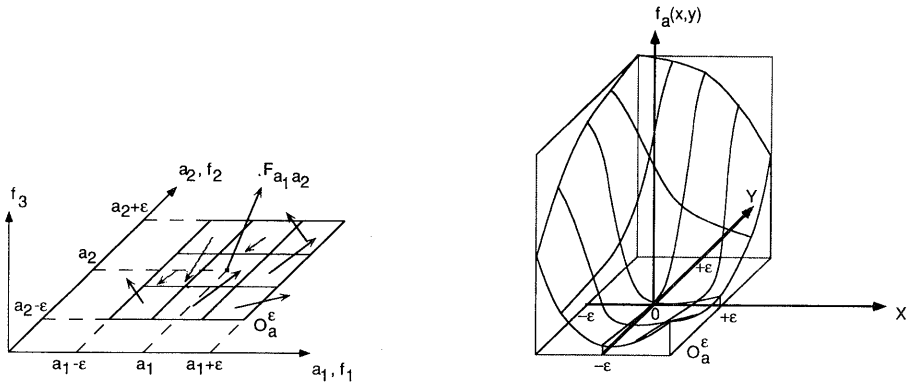

Fig. 3 Calculation of the sample function from texture sampling of an image.
Left: example of image texture sampling and the 3D feature vectors (f_1, f_2, f_3) in a O_a^ε neighborhood. Right: calculated graph of the sample function $f_a(x, y)$ defined for all $(x, y) \in O_a^\varepsilon$.

used as a similarity measure between texture features $F^i=(f_1{}^i, \cdots, f_7{}^i)$ and $F^j=(f_1{}^j, \cdots, f_7{}^j)$ with the following definition

$$\mu(F^i, F^j)=\sum_{k=1}^{7}\frac{(f_k^i-f_k^j)^2}{(f_k^i)^2+(f_k^j)^2}. \quad (7)$$

3. Texture Contour Model

We assume parametric representation of an active contour by $v(s)=(x(s), y(s))$, $0\leq s\leq 1$ and its minimized energy functional

$$E_{snake}=\int_0^1 E_{int}(v(s))+E_{texture}(v(s)) + E_{image}(v(s))ds. \quad (8)$$

The energies

$$E_{int}=\frac{1}{2}(w_1(s)|v'(s)|^2+w_2(s)|v''(s)|^2), \quad (9)$$

$$E_{image}=w_3 I(x, y)+w_4|\nabla(G_\sigma * I(x, y))|^2, \quad (10)$$

are internal and image energy, respectively; they are similar to the ones defined in Ref. 7). The functions $w_1(s)$, $w_2(s)$ and constants w_3, w_4 are appropriate selected weights, $G_\sigma *$, denotes convolution with a Gaussian smoothing filter of a width σ, and $\nabla(\cdot)$ is the gradient operator. The internal energy E_{int} imposes a piecewise smoothness constraint upon active contour $v(s)$ while image energy E_{image} pushes the active contour towards the lines and edges of an image.

New type of energy

$$E_{texture}=v_e E_{edge}+v_c E_{corner} \quad (11)$$

called texture energy has been incorporated, where v_e and v_c are constants.

In this section, we present two different tex-

Fig. 2 Extraction of a circle sampled by texture on a texture background.
Upper: given initial contour. Lower-left: final contour equilibrium obtained with texture edge energy only. Lower-right: contour equilibrium gained in the image space only.

Fig. 4 One example of a corner following.
Left: synthetic image with initial contour. Right: final contour on target shape attracting the triangle corners.

Fig. 5 The extraction of a circle contour when there exists poor contrast between circle and background.
Upper: synthetic image with roughly given initial contour. Lower-left: final contour of a circle received from texture information. Lower-right: contour in equilibrium received by scale space employing.

Fig. 6 Corners of the synthetic image of a linden leaf.
Upper: initial contour. Lower-left: final contour using discontinuities and texture. Lower-right: result contour from image scale space employing.

Fig. 7 Optical microscope image of a mouse embryo.
Upper-left: initial contours of the mouse embryo's stomach. Upper-middle: final contours of the stomach of the embryo using textures. Upper-right: result contours from image scale space. Lower: enlargement of selected areas from the upper images.

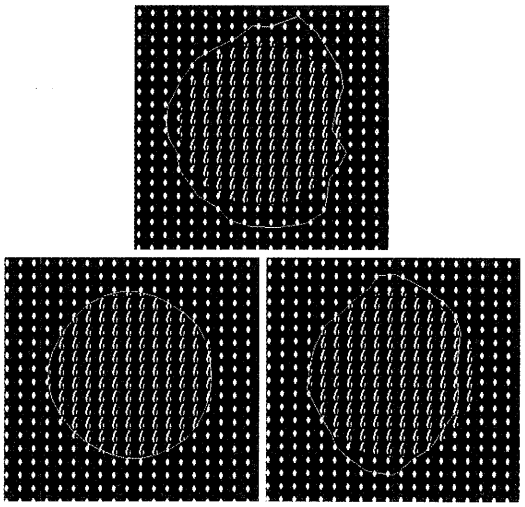

Fig. 2

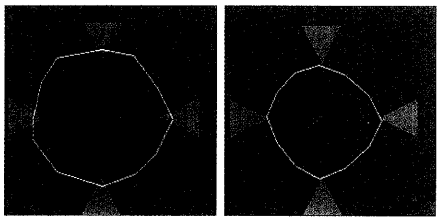

Fig. 4

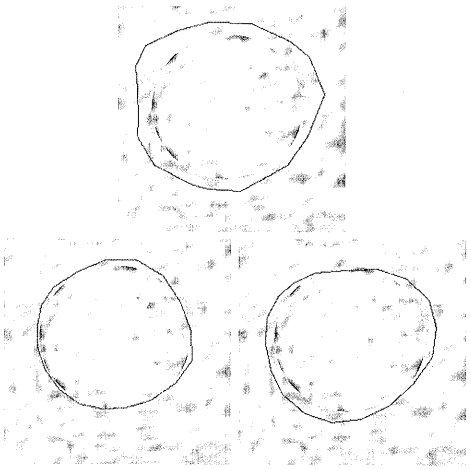

Fig. 5

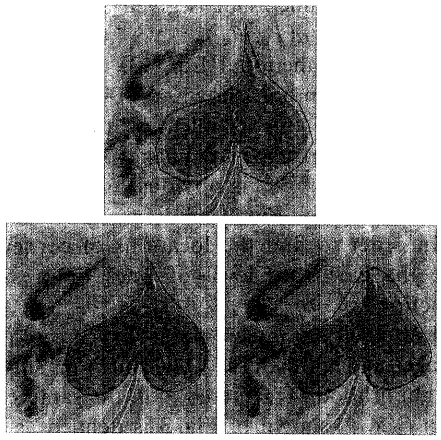

Fig. 6

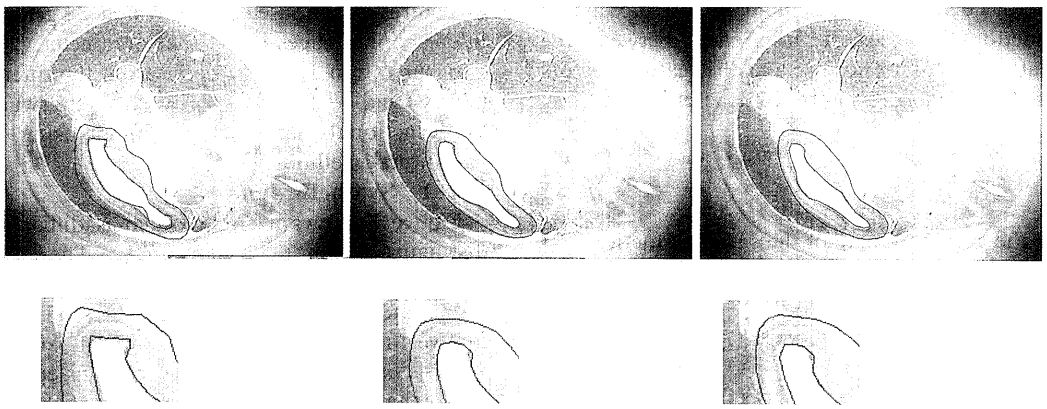

Fig. 7

ture energy functionals E_{edge} and E_{corner} which attract active contour $v(s)$ to the edges and corners of the image. To make these energies in function, we assume that for each point within the image, exactly one feature vector is given from the segmentation step.

3.1 Edge Functional

At each point of the active contour $v(s)$ we define a normal N_s to the contour in a point $v(s)$. One auxiliary point $V_n^+(s)$ is procured for the point $v(s)$, in order to introduce the edge functional. It is defined for the arbitrarily small constant $\xi>0$ as follows:

$$V_n^+(s)=v(s)+\xi N_s. \tag{12}$$

Let us denote F_n^+ and F_v as the texture feature vectors corresponding to both the auxiliary point V_n^+ and the contour point $v(s)$, respectively. The edge locations are places where feature vector V_n^+ varies sufficiently from vector F_v. Hence, edge functional is given by

$$E_{edge}=-\mu(F_v, F_n^+) \tag{13}$$

The edge functional Eq. (13) was used with the active contour shown in **Fig. 2**. The insolvability of this problem using only image space or scale space i.e. images smoothed by a Gaussian filter[7),3),8)] is obvious.

3.2 Corner Functional

In order to find the locations of corners, we use the curvature level of lines on a sample function.

For arbitrary given point $\boldsymbol{a}=(a_1, a_2)$ in the image and for all (x, y) within the small ε-neighborhood O_a^ε centered at $\boldsymbol{a}$, the sample function $f_a(x, y)$ shown in **Fig. 3** is defined as

$$f_a(x, y)=\mu(F_{a_1,a_2}, F_{x,y}). \tag{14}$$

The notation F_{a_1,a_2} denotes a texture feature vector corresponding to the point $\boldsymbol{a}$. The sample function describes the differences between the feature vector in point $\boldsymbol{a}$ and the feature vectors in a small neighborhood of $\boldsymbol{a}$. Let

$$\Phi=\tan^{-1}\left(\frac{\frac{\partial f_a}{\partial y}}{\frac{\partial f_a}{\partial x}}\right) \tag{15}$$

be the gradient angle of the sample function and let $\boldsymbol{t}=(-\sin\Phi, \cos\Phi)$ be a unit vector perpendicular to the gradient direction. Thus the corner functional is follows

$$E_{corner}=-\left(\frac{\partial\Phi}{\partial t}\right)^2 \tag{16}$$

The image shown in **Fig. 4** is a synthetic one with four triangle corners followed by active contour with usage of the corner functional Eq. (16).

3.3 Discontinuity Behavior

Discontinuities in the active contour $v(s)$ of the order $0\leq k<2$ will occur freely[12)] at a point $v(s_0)$ when coefficient $w_j(s_0)$ in Eq. (9) is set to 0 for all $j>k$. The second order continuity constraint will be ignored where the E_{corner} is greater than a threshold value. Thus the second order continuity constraint will be controlled by

$$w_2(s)=\begin{cases}0 & \text{if } E_{corner}>threshold\\ \text{constant} & \text{otherwise}\end{cases} \tag{17}$$

where $w_2(s)$ is coefficient in Eq. (9).

4. Experiments

The boundary finding system was investigated by testing on real and synthetic images. Unfortunately, a method for an automatic setting of parameters is unknown. We use to set parameters manually according to our experiences. When extracting contours from a series of microscopic images, we set all the parameters M, d, w_i, v_e, v_c once for each initial contour within the selected microscopic image. Afterwards, the same parameters are used for all images from the series of microscopic images.

The size of a small sample window (parameter M) forming feature vectors varies from 8 to 18 pixels and the step between samples (parameter d) from 4 to 9 pixels. Both depend on image quality. Usually, the elastic parameters w_1 and w_2 in Eq. (9) can vary within the interval (0, 1) while parameters w_3 and w_4 corresponding to the image energy, Eq. (10) fall in interval $(-1, 0)$. Structures of a mouse embryo which we get from microscopic images imply that parameter v_e and v_c occurring in Eq. (11) come from the interval $(-1, 0)$ and $(-5, 0)$, respectively. Afterwards, the functional minimum is found using the variational methods.[4)]

4.1 Synthetic Images

Figure 5 shows a circle which is difficult to distinguish from its background. The initial contour only roughly agrees with the target shape and the location. The extraction of feature vectors from samples of size 12×12 and step 4 pixels is achieved as a preprocessing step. The parameter v_c in Eq. (11) is set to zero because we don't have corners in this example and

parameter v_e can vary from -0.2 to -0.3. The final curve delineates the target with an approximately 1.1 pixel average error per contour point, while methods not using texture information[7),3)] sketch the target with one of 7.2.

Another synthetic image is shown in **Fig. 6**. The target is the shape of a linden leaf with a sharp corners. This form is described by a discontinuous contour. The background and the stem are potential sources of confusion. The final contour accurately describes the linden leaf and avoids the other objects.

4.2 Real Images

An active contour model using global shape information obtained from texture feature vectors has been applied to a variety of objects from real mouse embryo images taken by means of an optical microscope. The results of the method applied to the problem of depicting the stomach from these images are shown in **Fig. 7**.

5. Conclusions

A method has been described for faithfully following dynamic contour using a texture feature vector description. This work incorporates texture approach into active contour deformable models by definition of texture energies on edges and corners. It was found to reduce the difficulty when using active contour models in the case of both real and synthetic images and to be relatively insensitive to the problems of very concave boundaries and complex textures. When solving the problem of reconstruction from a set of contours extracted from a series of microscopic images, we do not need to set the parameters for each image in the series separately, it's sufficient to set then once for each initial contour within the selected image.

An area of further study in this work is the problem of multi-contour extraction. In the proposed model, the solution of the active contour model gives us contour position which is independent from positions of the other contours lying within the image area. Additional constraints between each pair of active contour, such as constraint between their centers can be introduced in our contour model to help in determining indistinguishable or broken boundaries.

Future orientation is extending the present model to dynamic surface models in 3D space.

Acknowledgements The authors wish to thank Prof. Mineo Yasuda and Prof. Akinao G. Sato for their advice and for providing the sample images and also to thank Prof. Tomoyuki Nishita for most helpful discussion.

References

1) Bajcsy, R. and Kovačič, S.: Multiresolution Elastic Matching, *Comput. Vision Gr. Image Process.*, Vol. 46, pp. 1-21 (1989).
2) Burr, D. J.: A Dynamic Model for Image Registration, *Computer Gr. Image Process.*, Vol. 15, pp. 102-112 (1981).
3) Carlbom, I., Terzopoulos, D. and Harris, K. M.: Reconstructing and Visualizing Models of Neuronal Dendrites, *Visual Computing* (ed. Kunii, T. L.), pp. 623-638, Springer-Verlag, Tokyo (1992).
4) Courant, R. and Hilbert, D.: *Methods of Mathematical Physics,* Vol. I, pp. 164-274, Interscience, London (1953).
5) Etoh, M., Shirai, Y. and Asada. M.: Contour Extraction by Mixture Density Description Obtained from Region Clustering, *Proceedings of the Second European Conference on Computer Vision,* Santa Margherita Ligure, Italy, pp. 24-32 (1992).
6) Kashyap, R. L. and Chellappa, R.: Estimation and Choice of Neighbors in Spatial Interaction Models of Images, *IEEE Trans. Inform. Theory,* Vol. IT-29, pp. 60-72 (1983).
7) Kass, M., Witkin, A. and Terzopoulos, D.: Snakes: Active Contour Models, *Proc. Int. Conf. Comput. Vision,* pp. 259-268 (1987).
8) Kita, Y.: Model-Driven Contour Extraction for Physically Deformed Objects—Application to Analysis of Stomach X-ray Images, *Proc. 11th IAPR International Conference on Pattern Recognition (Volume I),* IEEE Computer Society Press, Hague, pp. 280-285 (1992).
9) Mengyang, L., Jiamei, Q. and Yanni, T.: Texture Classification and Segmentation using Simultaneous Autoregressive Random Model, *Proc. of 5th Symp. on Computer-Based Medical Systems,* pp. 398-401 (June 1992).
10) Russ, J. C.: *The Image Processing Handbook,* pp. 101-136, CRC Press (1992).
11) Staib, L. H. and Duncan, J. S.: Boundary Finding with Parametrically Deformable Models, *IEEE Trans. Pattern Analysis and Machine Intelligence,* Vol. 14, No. 11, pp. 1061-1075 (1992).
12) Terzopoulos,D. and Fleischer, K.: Modeling

Inelastic Deformation : Viscoelasticity, Plasticity, Fracture, *Computer Graphics, (Proc. SIGGRAPH)*, Vol. 22, No. 4, pp. 269-278 (1988).
13) Wang, Y. F. and Wang, J. F. : Surface Reconstruction Using Deformable Models with Interior and Boundary Constraints, *IEEE Trans. Pattern Analysis and Machine Intelligence,* Vol. 14, No. 5, pp. 572-579 (1992).

(Received May 18, 1993)
(Accepted April 21, 1994)

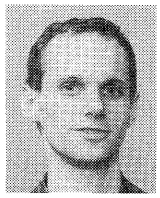

Roman Ďurikovič received the M. S. degree in numerical analysis from Comenius University, Bratislava, Slovakia, in 1989.

During the spring of 1991 he followed graduate courses in systems and control theory at the Groningen University, Netherlands. Since 1992 he joined as a visiting scholar, the computer graphics group of Hiroshima University, Japan.

He is currently a Ph. D. student in electrical engineering at this university. His research interests are image processing, computer graphics and physical modeling.

Kazufumi Kaneda received the BE, ME, and DE, from Hiroshima University, Japan, in 1982, 1984, and 1991, respectively. He worked at the Chugoku Electric Power Company Ltd. from 1984 to 1986. He is a research associate in Faculty of Engineering at Hiroshima University from 1986. He was also a visiting researcher in Engineering Computer Graphics Laboratory at Brigham Young University, USA, in 1991.

His research interests include computer graphics and image processing.

He is a member of ACM, IPS of Japan, IEE of Japan, and IEICE of Japan.

Hideo Yamashita received the B. E. and M. E. degrees in electrical engineering from Hiroshima University, Hiroshima, Japan, in 1964 and 1968, and Dr. of Engineering degree in 1977 from Waseda University, Tokyo, Japan. He was appointed as a Research Assistant in 1968 and an Associate Professor in 1978 of the Faculty of Engineering, Hiroshima University. Since 1992 he has been a Professor at Electric Machinery Laboratory, Faculty of Engineering, Hiroshima University. He was an Associate Researcher at Clarkson University, Potsdam, N. Y. in 1981-1982.

His research interests lie in the area of scientific visualization, computer graphics, and the magnetic field analyses by using the Finite Element Method and Boundary Element Method.

He is a member of the IEEE, the ACM, the IEE of Japan, the IECE of Japan, the IPS of Japan, the Japan Society for Simulation Technology, and the Japan Society of Applied Electromagnetics.